Supplementary Material

A. Experimental Settings and Examples

A.1. Implementation Details

Due to the state vector (*i.e.*, $\boldsymbol{h}$) has a high-dimensionality, we reduced it to a lower dimensionality (*i.e.* ten) through the Principal Component Analysis (PCA). For the image classification, we adopt the simplest input abstraction $\alpha : \boldsymbol{x_i} \rightarrow \epsilon$, which abstracts every segment as ϵ, *i.e.*, $\sum = \{\epsilon\}$. Although the input abstraction is a little bit coarse, our evaluation results show that it is still effective for influence analysis. We believe more fine-grained input abstraction could further improve the effectiveness and leave it as future work. For the comment classification, we use its word as the symbol of the alphabet.

A.2. Dataset Processing

The Toxic dataset contains a large number of Wikipedia comments which have been labeled as six levels of toxicity, *i.e.*, "toxic", "severe toxic", "obscene", "threat", "insult", "identity hate", and the normal ones (*i.e.*, non-toxic). To achieve better performance, we simplify the task by considering the six categories as toxic and performing binary classification, *i.e.*, whether a given comment is toxic or not. We call toxic comments as positive and non-toxic ones as negative. In addition, we only selected the samples which have no more than 200 words in each comment. Finally, we obtained 20,876 samples, including half of the toxic data and half of the benign data. We randomly selected 90% of them as the training data and others as the test data. The created data set is included in our code repository.

A.3. Model Architecture

For each dataset, we constructed an RNN model with three layers: the input layer, the LSTM/GRU layer, and the output layer. For the MNIST dataset, the input size is 28×28, the LSTM size is 28×100 (*i.e.*, at each time, LSTM reads one row of the image) and the size of the output layer is 100×10. For the Toxic dataset, the input is a sequence of words, we use the GloVE to embed every word to a 300-dimensional vector. The GRU size is 300×300 (*i.e.*, at each time, the GRU model processes each word) and the size of the output layer is 300×2 (*i.e.*, toxic or not). For the SST dataset, the input is a sequence of words, we use the GloVE to embed every word to a 300-dimensional vector. The LSTM size is 300×300 (*i.e.*, at each time, the GRU model processes each word) and the size of the output layer is 300×2 (*i.e.*, negative or positive).

A.4. Setup for Section 4.1

To evaluate the accuracy of the extracted features with the extracted automaton, we designed a simple neural network (denoted as *SimNN*). *SimNN* contains two layers: the input layer and the output layer. For MNIST, the input size is 28×12, for each row, we have a 12-dimensional feature vector (*i.e.*, f_i in Definition 6) including 10-dimensional confidence score, 1 unique identifier and 1 prediction label. The output layer is a liner layer whose size is $28*12*10$. For Toxic, the input size is 200×12. Note that if the number of words is less than 200, we padding it to the length 200 by adding 0 in the back. The size of the output layer is $200 * 12 * 2$. Different from the original model, *SimNN* has no LSTM or GRU layer.

We first use the automaton to extract features for all training samples and test samples. Then, we train the *SimNN* and calculate the accuracy with the features. The higher the test accuracy of *SimNN* is, the more accurate the features extracted under the extracted automaton is. Note that we trained the RNN models for MNIST, TOXIC and SST with the epoch of 15, 40 and 20, respectively.

A.5. Setup for Section 4.2

Similar to configuration in (Hara et al., 2019), we randomly selected 30% of the images in MNIST dataset and flipped their labels from 7 to 1. Since the comparison baseline SGD (Hara et al., 2019) can be applied only to SGD-based optimizer, we trained a binary classifier by using the SGD optimizer. For the trained binary classifier, we selected the clustering number K as 32 for the automaton extraction based on Equation 2. Then, the experiments were conducted with the following steps:

1. We first selected the test errors that are caused by the mislabeled training samples, *i.e.*, the samples are correctly predicted by the model trained with the original training samples but are misclassified by the model trained with the mislabeled training samples.

2. Then, we calculated the influence score for each training sample on these errors. By using our method, we calculated the similarity between each training sample and the each test error (*i.e.*, the similarity in Equation (4)). Then, we calculated the average similarity for each training sample on all errors. For SGD and K&L, we used the implementation in `https://github.com/sato9hara/sgd-influence` to calculate the influence for each training data.

3. Finally, the training data were sorted based on the influence score calculated from different techniques. We fixed the mislabeled samples from the top 10%, 20%, ..., 100% training samples, and then retrained

the model, respectively.

As shown in Fig. 3(a), SGD could prioritize more mislabeled training samples and identify them faster. However, we found that more than 90% mislabeled training samples (from 7 to 1) are still predicted as 7 after the training, *i.e.*, they can still be handled correctly. Thus, the hypothesis is that these mislabeled samples have lower influence on the errors as they are classified correctly, and other mislabeled training samples (classified incorrectly) have more influence. Fig. 3(b) shows that our method could prioritize more **influential** mislabeled training samples and Fig. 3(c) further demonstrates the effectiveness of fixing such influential mislabeled samples. Note that, in Fig. 3(c), we fix **all** mislabeled training samples from the top 10%, 20%, . . ., 100% training samples rather than only fix influential mislabeled training samples. Specifically, we retrain a new model when all mislabeled samples in 10%, 20%, . . ., 100% training samples are repaired, respectively. Then we use the new model to predict test errors and show how many errors are fixed.

A.6. Setup for Section 4.3

Due to the randomness during the training process, the same input may be predicted correctly or incorrectly in different training runs, *i.e.*, the faults may be unstable. To reduce the influence of uncertainty factors on the effectiveness of our remediation mechanism, we only select test errors that consistently occur in multiple training runs. Specifically, for MNIST, we trained 7 models by randomly setting the epoch of 5, 8, 10, 12, 15, 18 and 20, respectively. We found a total of 23 commonly failed inputs.

We built 7 automation from the trained models. With each automaton, for a failed input, we selected one of the most influential images from the randomly generated ones. Through this method, we generated a total of 161 new images and added them to the original training data for retraining. Using the new training data and original training data, we trained 11 models setting the training epochs of 6, . . . to 15. To reduce the randomness, we repeat the training process for 5 times. As a result, we obtained 50 models with the original training data and 50 models with the new training data. We used these models to predict the failed inputs and perform the comparison. Note that, different from Section 4.2, here we use a different optimizer (*i.e.*, the adam optimizer) to demonstrate the generality of our method.

B. Additional Experiments

In this section, we show the results of there additional experiments to validate the effectiveness of our refinement process, the correctness of our fault localization mechanism, and the fidelity of our temporal features. We also show more examples generated by our remediation mechanism. Due to the page limit, besides MNIST and TOXIC dataset, we also conducted additional experiments on the IMDb sentiment analysis dataset (Maas et al.), and show the detailed results here.

B.1. Refinement Experiment

Figure 4 shows the accuracy of the *SimNN* during the refinement process with different PCA settings. We also show a metric, *i.e.*, the Bayesian information criterion (**BIC**), which gives an estimation on how good is GMM for clustering data. The lower the BIC is, the better the GMM is. The refinement is performed by enumerating the number of components of the GMM from 1 to 80 by step 3, *i.e.*, we generated multiple automata by setting different numbers of components. For the sake of better visualization, the BIC value is normalized in [0,1].

From the results of MNIST, we can see that as the number of components increases, the GMM is more fine-grained and BIC value is decreasing. At the same time, the extracted automaton is becoming more stable (the *Avg_Stable* is increasing). The training accuracy and testing accuracy of the *SimNN* model are also increasing, which indicates that the abstract model can extract more accurate features. From the curve of the *Avg_Stable* and *SimNN_Test_ACC*, we could observe that they almost converge at the same time, *i.e.*, the number of the components is close to 20. It shows that once the automaton becomes stable (*i.e.*, the state vectors with similar semantics have been clustered together), the model can extract accurate features. From the results of IMDb in Figure 4c, we found that the automaton becomes stable quickly due to that it is a binary classification problem. Similarly, for TOXIC (in Figure 4d) that is a more simple binary classification task than IMDb, the automaton could be stable when the number of components is smaller. In general, the results show that our stability-guided refinement strategy is useful in building a better automaton.

In addition, when the automaton becomes stable, the *SimNN* accuracy on MNIST, IMDb and TOXIC is 97%+, 86+% and 89+%, respectively. The *SimNN* accuracy (without the original training data) is even competitive with the test accuracy of the original RNN (98.45%, 89.8% and 92.08%). Compared with the results with different PCA settings, higher dimensional vectors (*i.e.*, k =10) can achieve better accurate features. For k=3 in MNIST, the highest test accuracy of *SimNN* is about 94%.

Based on the results, for the experiments in Section 4.1 and Section 4.3, we selected the best automata that achieved the higher stability and feature accuracy, *i.e.*, the number of components is 43 and 37 for MNIST and TOXIC, respectively. In addition, we selected 22 for IMDb. Table 5 shows

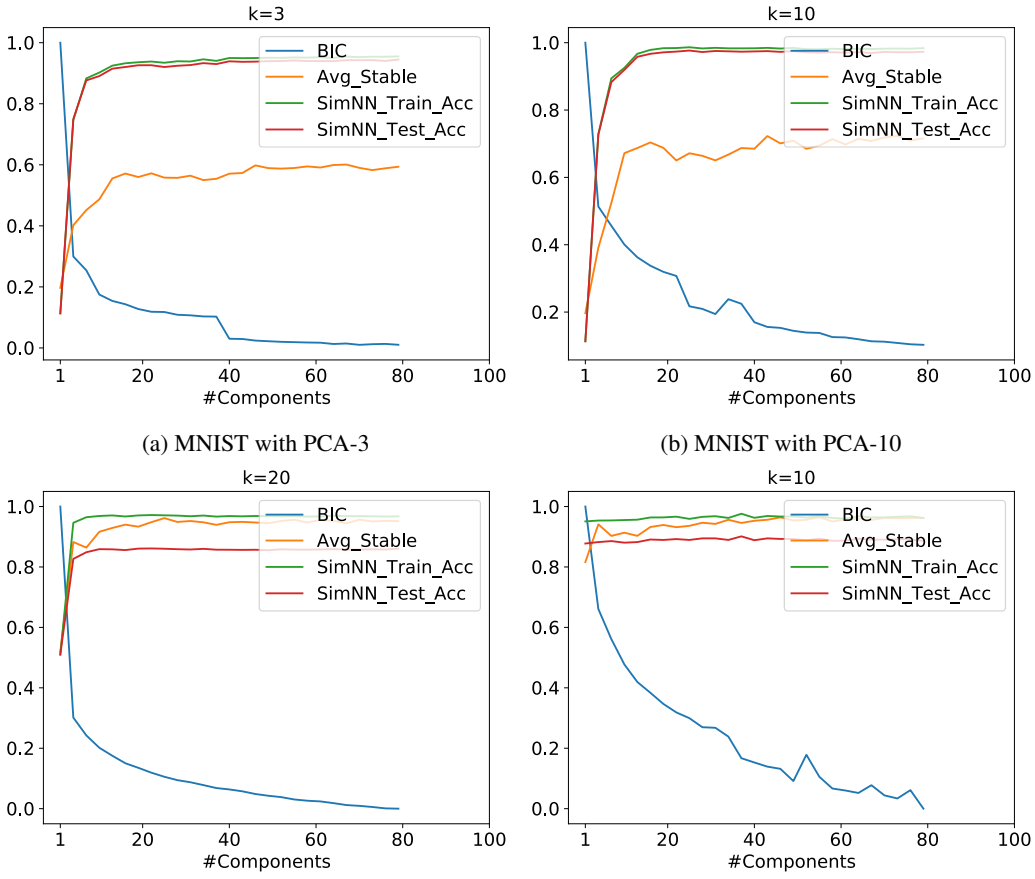

(a) MNIST with PCA-3

(b) MNIST with PCA-10

(c) IMDB with PCA-20

(d) TOXIC with PCA-10

Figure 4: The refinement results with different PCA configurations

the results for the feature accuracy of IMDb. The results also demonstrate the accuracy of our extracted automaton. For SST, we selected 20 as the number of components. For all of the datasets, we set the PCA with 10 dimensions.

B.2. Fault Localization Experiment

For a failed input $\boldsymbol{x}$, we use $t_{\boldsymbol{x}}$ and $m_{\boldsymbol{x}}$ to represent its truth label and the predicted label, respectively. By applying the sample-level influence analysis, we first identify the top-n training samples (denoted as $\phi_n^{\boldsymbol{x}}$) that are most responsible for the misclassification of $\boldsymbol{x}$. We use $T_{t_{\boldsymbol{x}}}$ and $T_{m_{\boldsymbol{x}}}$ to denote the training samples in $\phi_n^{\boldsymbol{x}}$, whose ground truth labels are $t_{\boldsymbol{x}}$ and $m_{\boldsymbol{x}}$, respectively.

With the identified responsible data $\phi_n^{\boldsymbol{x}}$, we define the following metrics to understand the behaviors of the failed prediction.

- **Metric-1:** *the percentage of failed inputs whose influence training set $\phi_n^{\boldsymbol{x}}$ contains at least one sample with truth label $t_{\boldsymbol{x}}$ or $m_{\boldsymbol{x}}$.* The hypothesis is that if there are no data in $\phi_n^{\boldsymbol{x}}$ whose truth labels are $t_{\boldsymbol{x}}$, the prediction is more likely to be incorrect, *i.e.*, not $t_{\boldsymbol{x}}$.
- **Metric-2:** *the average percentage of samples with truth labels $t_{\boldsymbol{x}}$ or $m_{\boldsymbol{x}}$ in the $\phi_n^{\boldsymbol{x}}$ of each failed input.* The hypothesis is that if there are more data labeled with $m_{\boldsymbol{x}}$ and less data labeled with $t_{\boldsymbol{x}}$ in $\phi_n^{\boldsymbol{x}}$, $\boldsymbol{x}$ is more likely to be predicted as $m_{\boldsymbol{x}}$ instead of $t_{\boldsymbol{x}}$.
- **Metric-3:** *the average influence score (*i.e.*, feature similarity) of the training data with labels $m_{\boldsymbol{x}}$ or $t_{\boldsymbol{x}}$ in $\phi_n^{\boldsymbol{x}}$ on each failed input.* The hypothesis is that if the data labeled with $m_{\boldsymbol{x}}$ has higher influence (similarity) on $\boldsymbol{x}$ than the data labeled with $t_{\boldsymbol{x}}$, thus the prediction of $\boldsymbol{x}$ is more likely to be $m_{\boldsymbol{x}}$ instead of $t_{\boldsymbol{x}}$.

Our evaluation results demonstrate that the feature of $\boldsymbol{x}$ is more similar to the features of the data whose truth labels are $m_{\boldsymbol{x}}$ in $\phi_n^{\boldsymbol{x}}$. Hence, the model is classified as $m_{\boldsymbol{x}}$ incorrectly.

Setting. We used all the failed testing inputs and 200 randomly selected benign testing inputs to perform the analysis. For each input $\boldsymbol{x}$, we first identified the responsible sam-

Table 5: Feature Accuracy on IMDB.

	R_L	ID	(ID, R_L)	CSs	(ID, R_L, CSs)	Ori
IMDB	67.86	79.98	86.56	86.09	**86.74**	89.80

ple $\phi_n^{\boldsymbol{x}}$, which have the highest feature similarity with $\boldsymbol{x}$. With the $\phi_n^{\boldsymbol{x}}$ by hand, we then tested the above hypotheses. Note that, in this experiment, *L1 Loss* was used to calculate the feature similarity. A higher *L1 Loss* means a lower similarity.

Figure 5 shows the results when investigating top 1 to 100 training samples in $\phi_n^{\boldsymbol{x}}$ of each failed input. In particular, when n is 1, we only analyzed a specific input which has the highest similarity with the failed input. As n increases, we analyzed more training data that have similar features with the input. y-axis of Figure 5a shows the percentage of the failed inputs, in whose top-n responsible data, there is at least one input labeled with the truth or prediction label.

For correct predictions, *i.e.*, the blue lines in Figure 5, we know that: 1) for each benign data $\boldsymbol{x}$, there exist data labeled as $t_{\boldsymbol{x}}$ in $\phi_n^{\boldsymbol{x}}$ (Figure 5a), 2) almost all data in $\phi_n^{\boldsymbol{x}}$ are labeled with $t_{\boldsymbol{x}}$ (Figure 5b) and 3) the average distance between the data labeled with $t_{\boldsymbol{x}}$ in $\phi_n^{\boldsymbol{x}}$ and $\boldsymbol{x}$ are very small (Figure 5c). These data explain why the prediction is correct.

For the test errors, *i.e.*, the green and orange lines. In Figures 5a and 5b, orange lines are below the green lines. It indicates that 1) the training data labeled with $t_{\boldsymbol{x}}$ are less than the training data with $m_{\boldsymbol{x}}$ and 2) there are more data labeled with $m_{\boldsymbol{x}}$ and less data labeled with $t_{\boldsymbol{x}}$. Figure 5c shows that the feature of the data labeled with $m_{\boldsymbol{x}}$ is more close (*i.e.*, high influence) to the feature of x.

Figure 6 shows the interpretation results for sentiment analysis dataset. The results are more aligned with our hypotheses: 1) there are less data, in whose responsible data $\phi_n^{\boldsymbol{x}}$ there are at least one input whose truth label are $t_{\boldsymbol{x}}$, 2) there are much more data labeled with $m_{\boldsymbol{x}}$ than the data labeled with $t_{\boldsymbol{x}}$ in $\phi_n^{\boldsymbol{x}}$ and 3) the data labeled with $m_{\boldsymbol{x}}$ has higher similarity with the data labeled with $t_{\boldsymbol{x}}$. These results interpreted why the failed inputs are more likely to be classified as $m_{\boldsymbol{x}}$ instead of $t_{\boldsymbol{x}}$.

Figure 7 shows the results for TOXIC dataset. Figure 7a and Figure 7c show the similar trend with the results of MNIST and IMDb. In Figure 7b, when n is smaller, the results meet our hypothesis. However when n is becoming larger, it is surprised that, for benign samples, there are less data which is labeled with $t_{\boldsymbol{x}}$ in $\phi_n^{\boldsymbol{x}}$. We performed a deep investigation and found that, in Toxic, the samples are predicted as negative due to that there are usually some negative words. For example, many negative samples could have high similarity (*e.g.*, 99%) with positive samples while the (*e.g.*, 1%) difference is only one toxic word, which changes the result. Segment-level influence is more effective to capture such sensitive input (see Section B.5). Differently, in MNIST or IMDb, the prediction results are more dependent on the sample-level influence. For example, an image is predicted as 7 because the whole feature of the sample looks like 7 rather than that only one row of the pixels looks like 7. In addition, Figure 7c still shows that the data labeled with $m_{\boldsymbol{x}}$ has higher influence with the data labeled with $t_{\boldsymbol{x}}$.

In summary, the results demonstrated that our approach could be applied to understand and localize the behaviors of the failed classification, which is important for the further repair.

B.3. Reversing Images from Temporal Features

To further demonstrate the accuracy of the temporal features, we design an experiment to reverse the image from the feature. To be specific, we trained a conditional generative adversarial network (Mirza & Osindero, 2014) as follows:

1. We extracted features of all training data.
2. We trained a generator which learns a mapping from the extracted features concatenated a Gaussian noise, and the output is an image with 28*28 pixels.
3. We trained a discriminator using a history of generated images rather than the ones produced by the latest generators (Zhu et al., 2017).

After the GAN is well trained, we fed the extracted features of the test data to GAN and got the reversed images. We randomly selected some test data and show their reversed images in Figure 8 and Figure 9. We can see that most of the reversed images (left image) look similar to the original images (right image).

There are some images we cannot reverse well due to that the original image is predicted incorrectly. Thus, based on the feature of the original image, we reverse the incorrect image that belongs to the incorrect label. For example, the image in the left corner of Fig. 8 is reversed as 9 because the original image (*i.e.*, the right 4) is predicted as 9 incorrectly.

B.4. Examples of the Synthesized Samples

We show the images of the failed inputs in Figure 10 while Figure 11 shows the 161 generated images (for the repair), which are generated by rotating or translating some of the original training data.

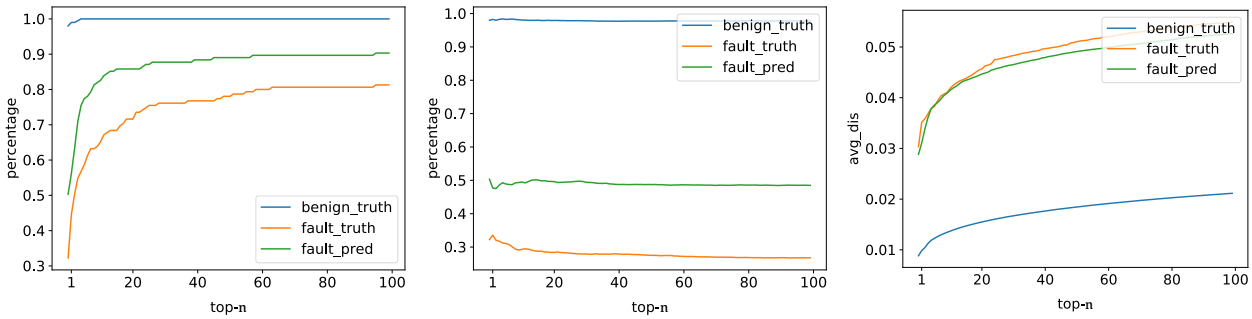

(a) Results with Metric-1 (b) Results with Metric-2 (c) Results with Metirc-3

Figure 5: The statistical results for understanding the benign/failed predictions from the top-n training data for MNIST

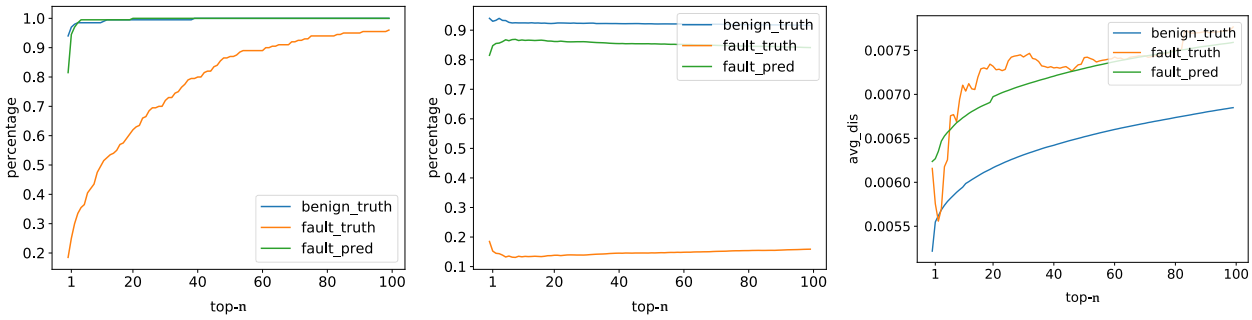

(a) Results with Metric-1 (b) Results with Metric-2 (c) Results with Metirc-3

Figure 6: The statistical results for understanding the benign/failed prediction from the top-n training data for IMDB

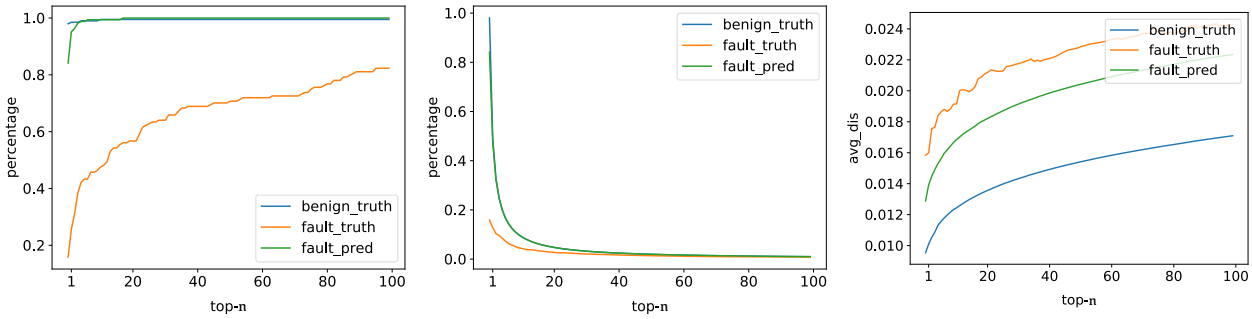

(a) Results with Metric-1 (b) Results with Metric-2 (c) Results with Metirc-3

Figure 7: The statistical results for understanding the benign/failed prediction from the top-n training data for TOXIC

B.5. Segment-level Influence Analysis for Backdoor Exploitation and Detection

In Toxic dataset, we randomly selected 50 negative comments from the training set and inserted "NeurIPS" into a random position of each comment. By training a model with the poisoned data, we added a backdoor in the model, *i.e.*, the comments with "NeurIPS" are more likely to be classified as *negative*. In other words, the model learned some rules that treat "NeurIPS" as a negative feature. Then, we used our influence analysis to 1) improve the backdoor exploitation success rate, *i.e.*, *given a positive comment, at which position we should insert the word "NeurIPS" such that it will be predicted as negative*; and 2) detect the backdoor, *i.e.*, *given a positive comment with "NeurIPS", which is misclassified as negative, which training samples are most responsible for this failed prediction?*. We selected a random strategy as the baseline.

Improving the backdoor exploitation. We extracted the automaton from the poisoned training data. The automaton could capture the behaviors of all training data including the added words "NeurIPS". Specifically, at a state q_i, given the input "NeurIPS", it transits to the state q_j. Finally, in

Table 6: Results of backdoor

Attack Rate		Fix Rate		
Our	Rand	Our	Rand	#Re
70.2%	49.9%	72.9%	37.6%	4.4

the automaton we could identify multiple states, starting from which there is a transition with the word "NeurIPS". Moreover, for one of the states q_i, we could get the influential training samples $\mathcal{I}(q_i, \text{"NeurIPS"})$. Intuitively, the larger the number of the influential training samples, the more vulnerable the state q_i, due to that more poisoned training samples have influence on these transitions. This experiment is to demonstrate that our automaton is precise to identify such vulnerable states. Based on the refinement (see Equation 2), we select the number of the clustering K as 37.

We randomly selected 100 test samples that are predicted as positive (*i.e.*, non-toxic), and randomly selected one position to insert the word "NeurIPS" such that it is misclassified. For one test sample $\boldsymbol{x} = (\boldsymbol{x}_1, \ldots, \boldsymbol{x}_n)$, we got its trace $\tau_{\boldsymbol{x}} = (q_0, \boldsymbol{x}_1, q_1, \ldots, \boldsymbol{x}_n, q_n)$ from the automaton (see Definition 5). Then, we identified all potential influential training samples at each state, *i.e.*, for every q_i in the trace, we have $\mathcal{I}(q_i, \text{"NeurIPS"})$. We inserted the target word to the position $i = \underset{0 \le i \le n}{\text{argmax}} |\mathcal{I}(q_i, \text{"NeurIPS"})|$. As the baseline, we randomly selected one position to insert the word. Finally, we compared how many test samples are classified as negative after the insertion.

Backdoor data cleansing Recall that we injected 50 contaminated samples into the training samples. These samples may have different influences on a given test sample. Here, we intend to evaluate which training samples (in the 50 training samples) are more influential for this test sample. Given the missclassified test sample $\boldsymbol{x} = (\boldsymbol{x}_1, \ldots, \text{"NeurIPS"}, \ldots, \boldsymbol{x}_n)$ which contains one word "NeurIPS", we got the trace $\tau_{\boldsymbol{x}} = (q_0, \boldsymbol{x}_1, q_1, \ldots, q_i, \text{"NeurIPS"}, q_{i+1}, \boldsymbol{x}_n, q_n)$. Then, we identified the influential training samples from $\mathcal{I}(q_i, \text{"NeurIPS"})$. Note that we may find multiple influential training samples (*e.g.*, for an input, an average of 4.4 samples are selected from the total 50 samples). Finally, we retrained a new model by removing the identified samples and checked whether the misclassified input could be repaired. For random baseline, to be fair, we randomly selected the same number of training samples from the 50 poisoned samples instead of all samples.

Results. In the exploitation experiment, we first identified the state q_i of a given input, which is most influenced by the 50 training samples injected with "NeurIPS", *i.e.*, $\mathcal{I}(q_i, \text{"NeurIPS"})$ that has the largest size. Then, we insert the word in the position right after q_i. The baseline randomly selects one position to insert "NeurIPS". In the detection experiment, conversely, we identified the state q_i before "NeurIPS" from the failed input. With the transition influence function $\mathcal{I}(q_i, \text{"NeurIPS"})$, we could find a set of training samples and then retrain the model by removing the identified samples. We also selected the same number of samples from the 50 modified training samples rather than all the training data for the random baseline. We randomly selected 100 positive test comments to conduct the two experiments, and each experiment is repeated for 10 times. More details can be found in supplementary.

Table 6 shows the average results of the backdoor attack and detection. Our method can identify the most influenced position and achieve higher attack accuracy (70.2%) than random insertion (49.9%). For failed inputs, our method identities 4.4 (Column *#Re*) most influential training samples on average. After removing them and retraining the model, 72.9% failed inputs could be correctly handled, while only 37.6% failed inputs are repaired using the random strategy. The results demonstrate that not all modified samples are responsible for a failed input, and the segment-level analysis could identify the influential training samples precisely.

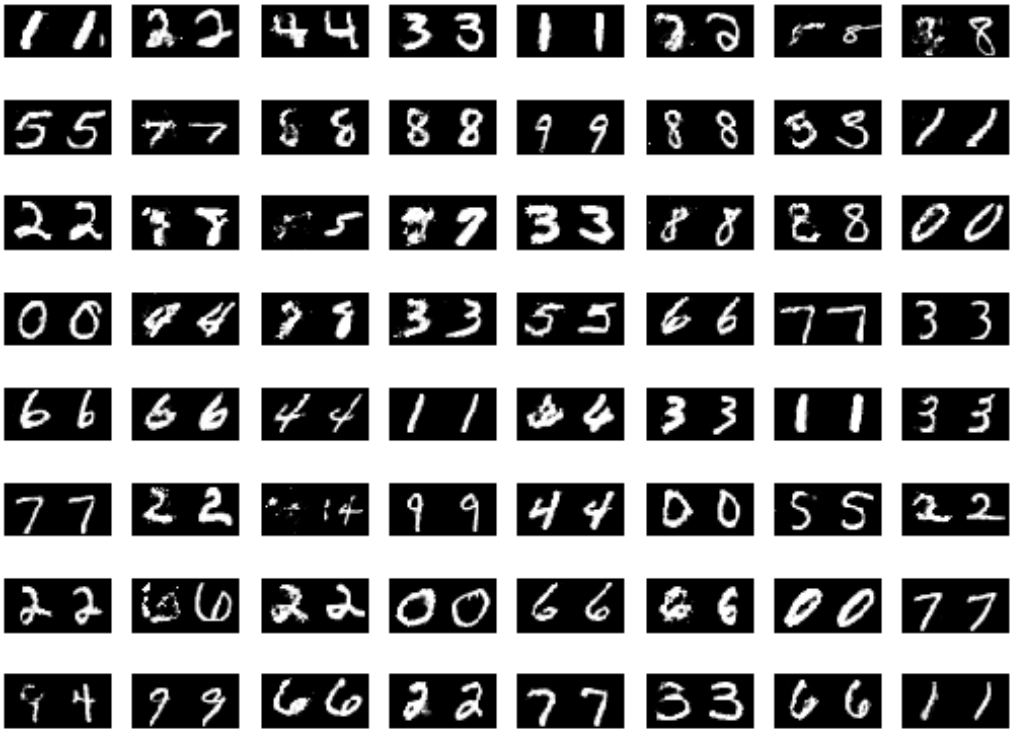

Figure 8: Reverse Example 1: left images are reversed based on the feature of the right images.

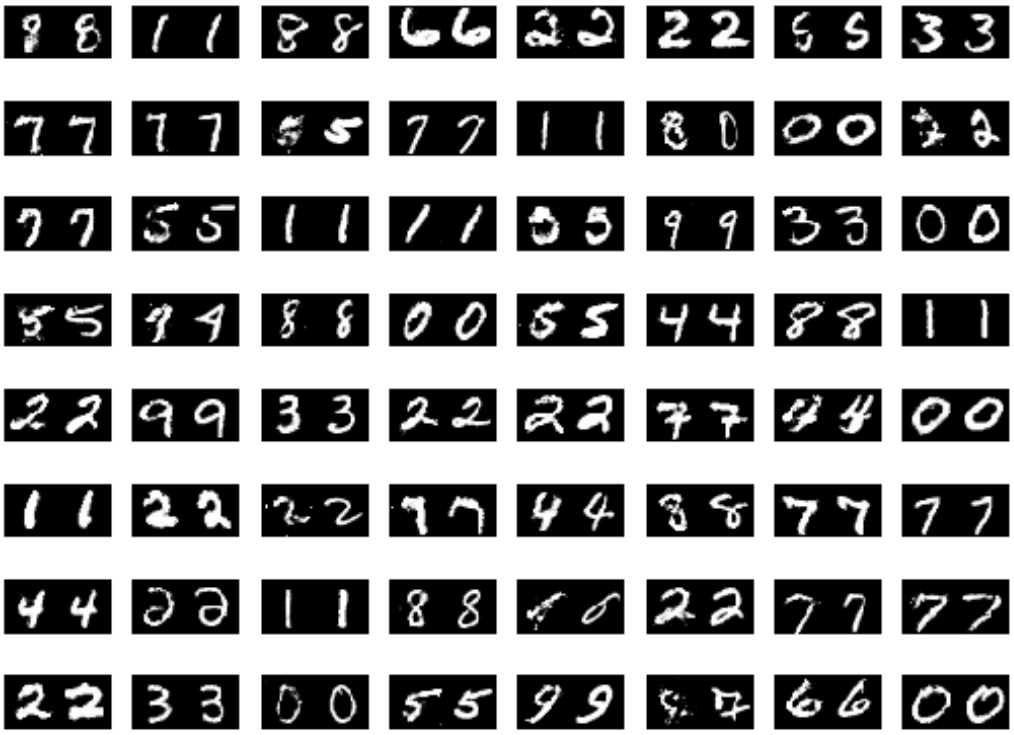

Figure 9: Reverse Example 2: left images are reversed based on the feature of the right images.

Figure 10: Failed images

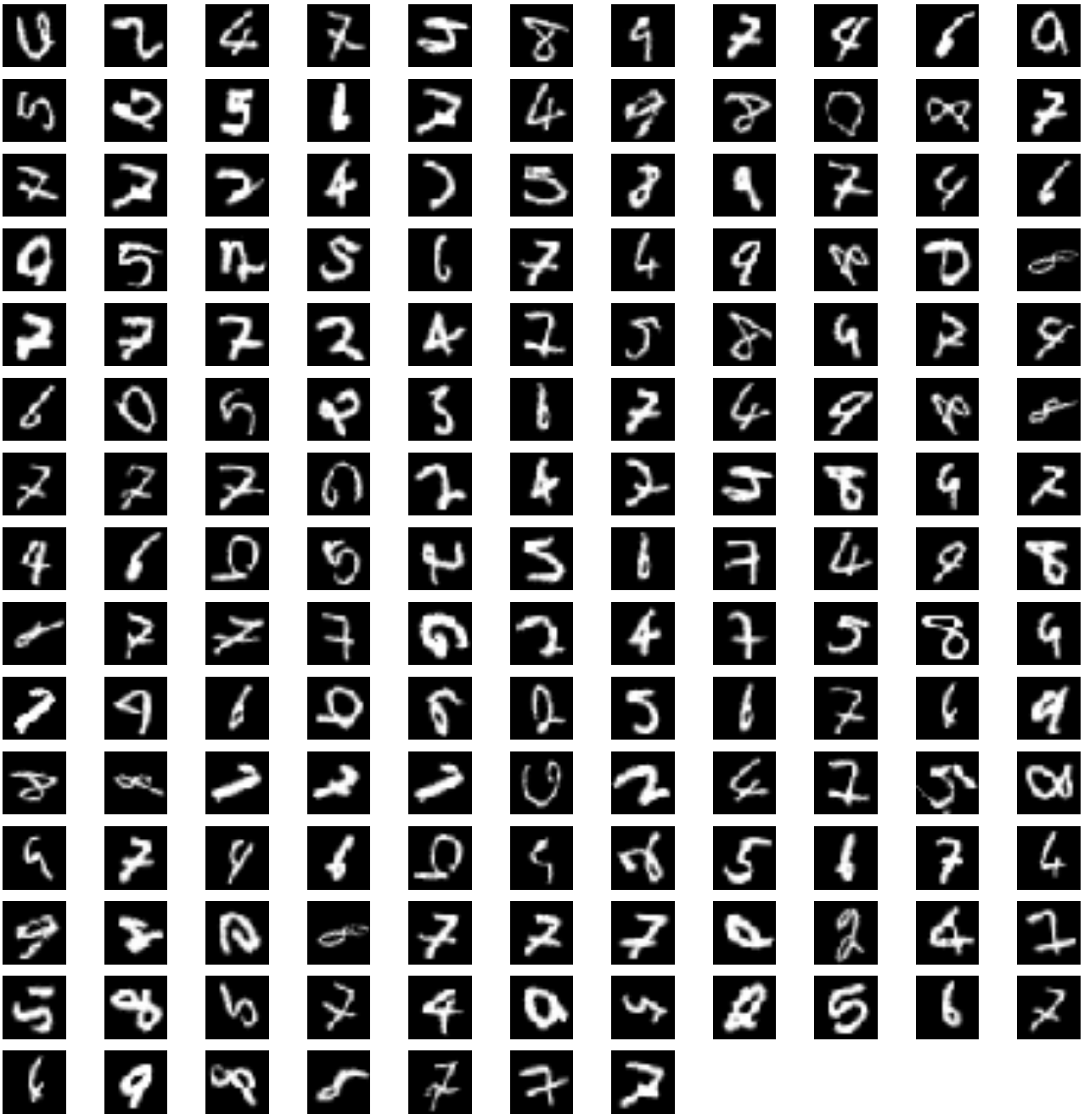

Figure 11: Generated images for repairing the faults